Vertical coupling and transport in high-latitude ionosphere

Dimitry Pokhotelov

with contributions from F. Günzkofer, I. Fernandez-Gomez, H. Sato, C. Borries, and N. Jakowski

Institute for Solar-Terrestrial Physics
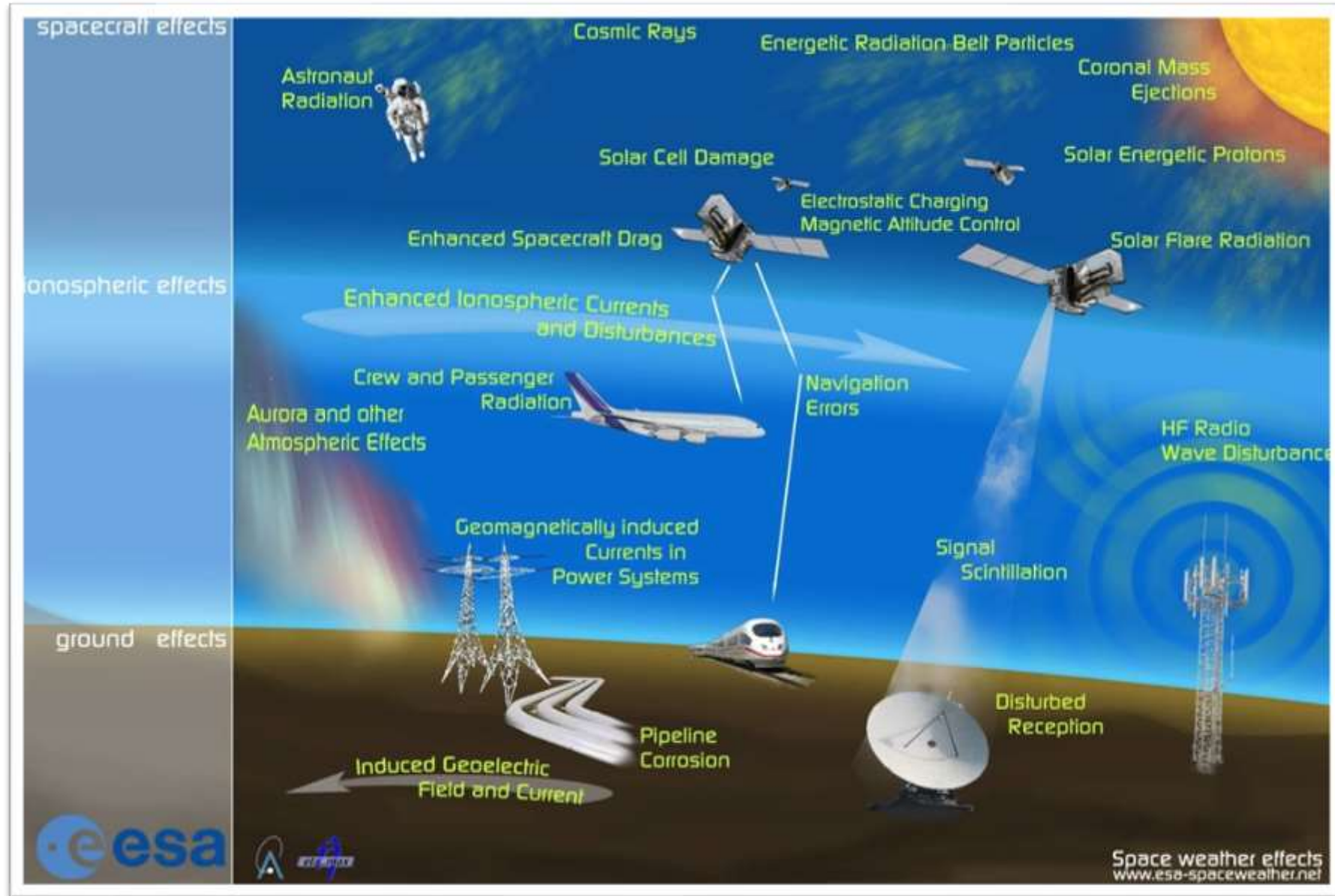German Aerospace Centre (DLR), Neustrelitz

Seminar at the GFZ
Potsdam, 6-Sep-2022

Knowledge for Tomorrow

Intro: Space weather

Ionospheric effects on GNSS

The ionosphere causes major problems for GNSS navigation:

Group delay to the signal propagation time that is proportional to the total electron content. This can change the apparent position by tens of metres.
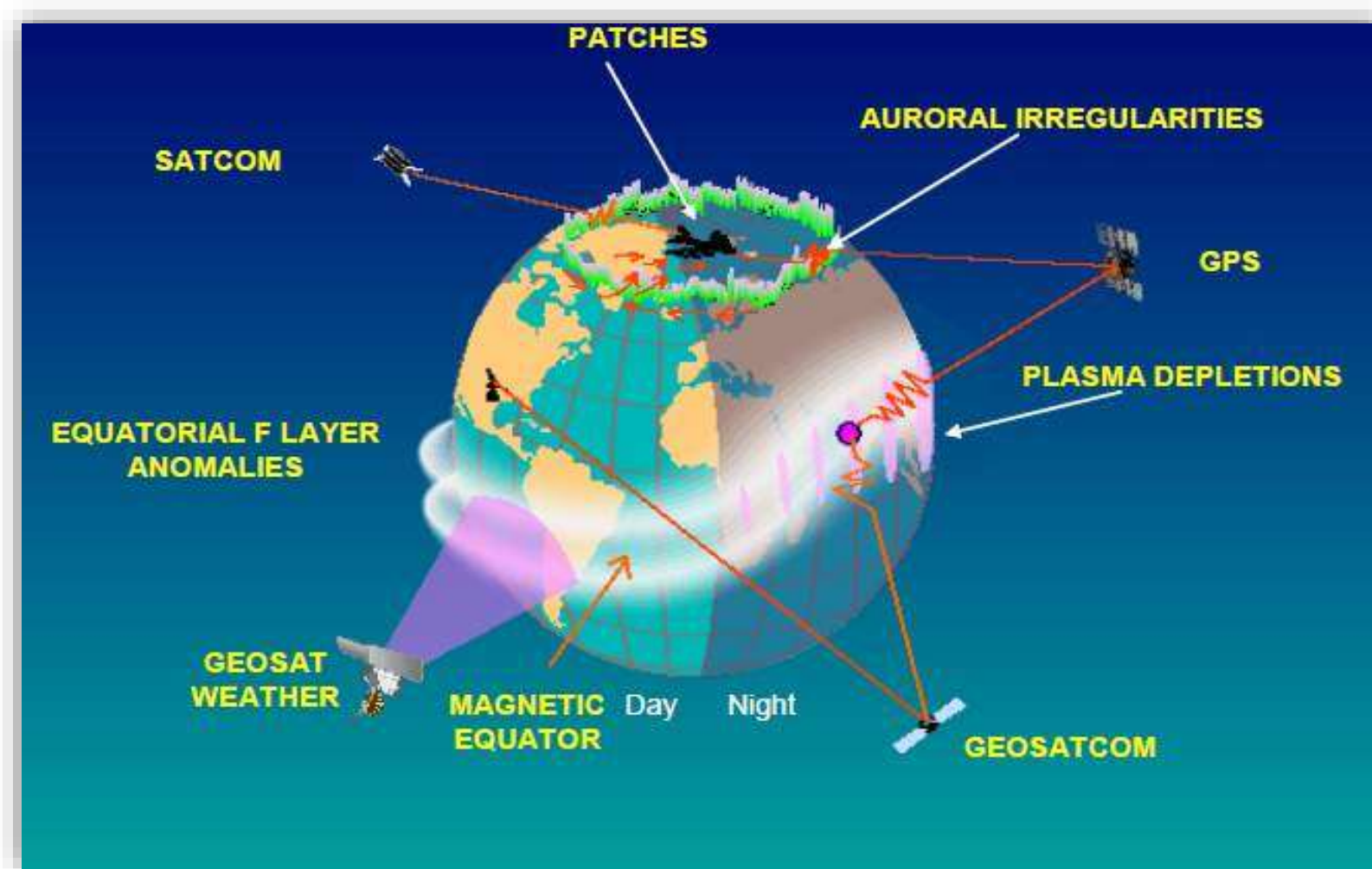
Scintillations of the signal are related to small-scale irregularities in plasma density. These can cause temporary loss of the signals.

 While these effects may not be an issue for most GNSS users but they are important for safety-critical applications.
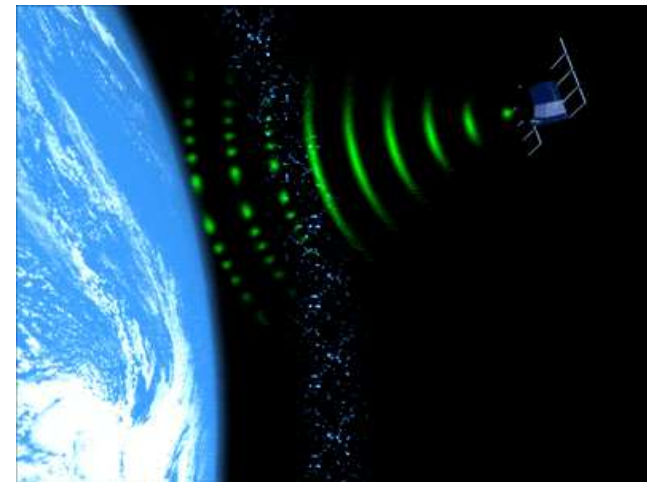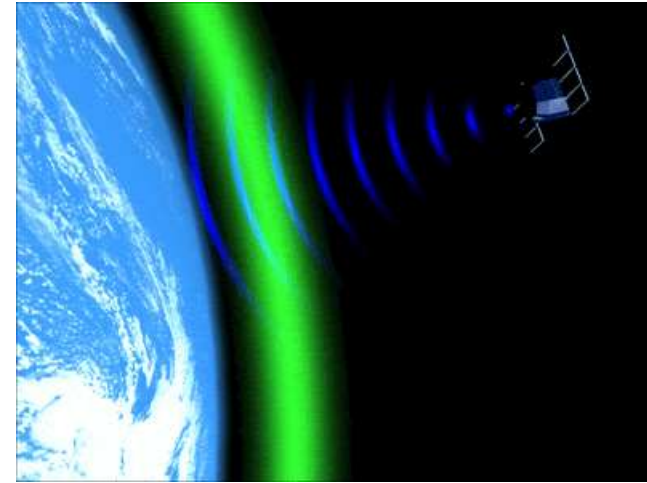
Credit: Univ. of Bath
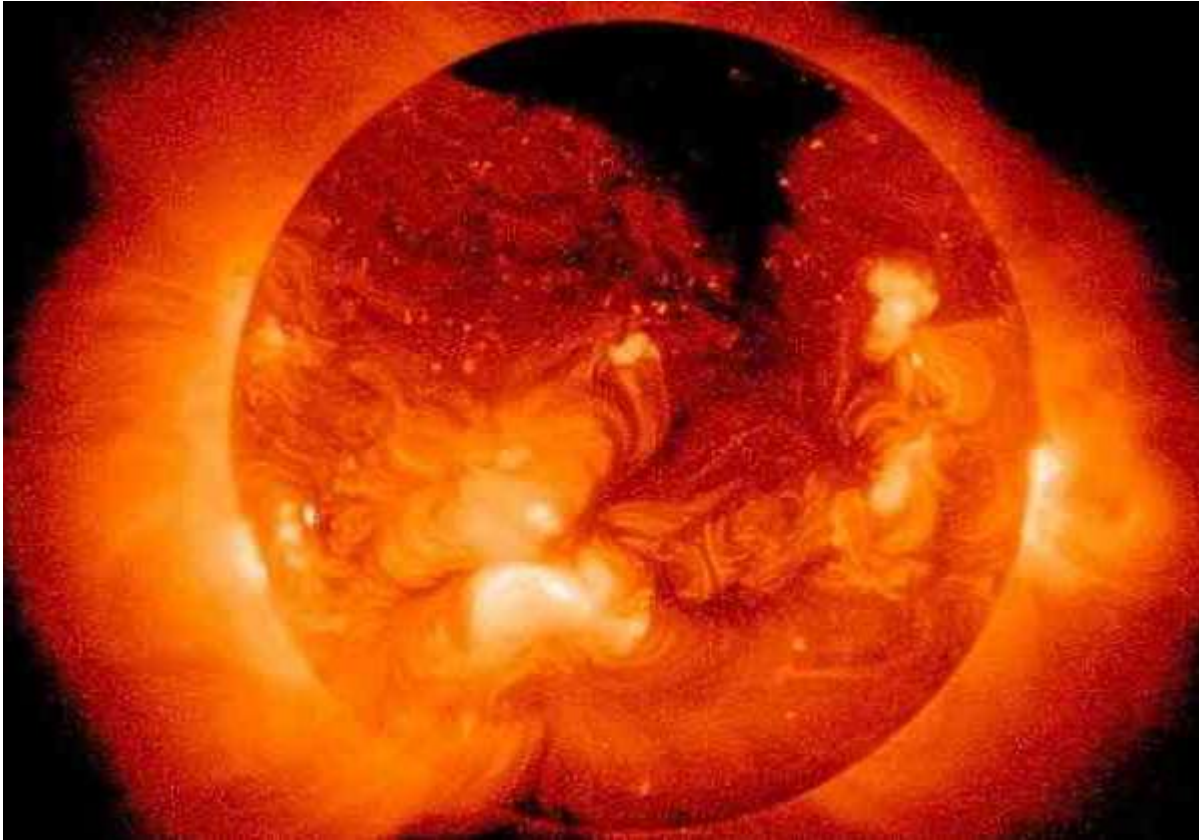
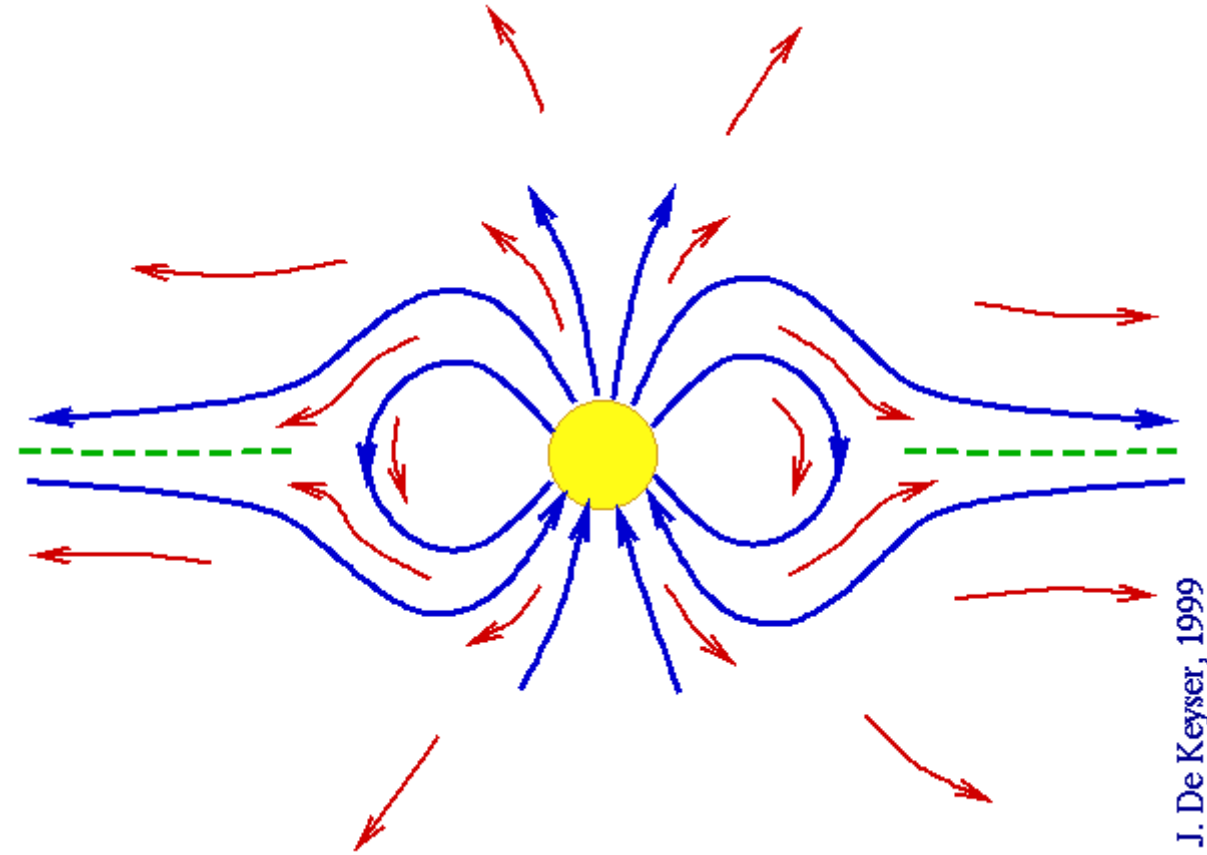# Global SatCom Outage Regions

Courtesy of H.C. Carlson

Origins of solar wind and interplanetary magnetic field (IMF)

Two distinct regions of the solar corona:

- Equatorial latitudes.

- Polar latitudes: coronal holes.

SOLAR-A probe image, courtesy of NASA

J. De Keyser, 1999

Diffusion and frozen flux

Assumptions:

- magnetised plasma;

- collisionless plasma (collision frequencies are much less than gyrofrequency, but not fully negligible);

- "cold" or "warm" plasma (particle energies substantially below relativistic, ~10s - 100s of eV).

From Faraday's law and generalised Ohm's law, eliminating **E** field:

$$\frac{\partial \mathbf{B}}{\partial t} = \nabla \times (\mathbf{v} \times \mathbf{B} - \mathbf{j}/\sigma_0)$$

Using $\nabla \cdot \mathbf{B} = 0$ and neglecting displacement currents (as usual in plasma physics):

$$\frac{\partial \mathbf{B}}{\partial t} = \boxed{\nabla \times (\mathbf{v} \times \mathbf{B})} + \boxed{\frac{1}{\mu_0 \sigma_0} \nabla^2 \mathbf{B}}$$

Advection term   Diffusion term

Magnetic diffusion

Assumptions:

- plasma at rest (or moving with constant velocity);

- conductivity is finite.

$$\frac{\partial \mathbf{B}}{\partial t} = D_m \nabla^2 \mathbf{B}$$ <- only diffusion term left

with the magnetic diffusion coefficient: $D_m = (\mu_0 \sigma_0)^{-1}$

Solution is given by: $B = B_0 \exp(\pm t / \tau_d)$

with the magnetic diffusion time: $\tau_d = \mu_0 \sigma_0 L_B^2$
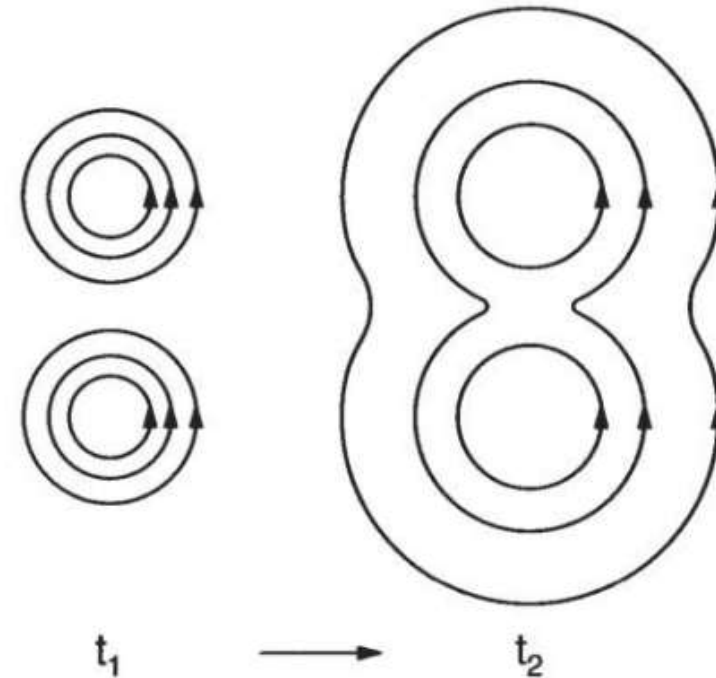
Consider typical solar wind:

    Density ~5 cm^{-3}

    Temperature ~50 eV

$$\sigma_0 = \frac{n_e e^2}{m_e \nu_c}$$

t_1 $\longrightarrow$ t_2

For the travel time from Sun to Earth (~ 3 days)

$$L_B \sim 10^3 \text{ m}$$

In solar wind the magnetic diffusion is negligible!

DLR

Frozen-in condition

Assumption:

- collisionless plasma with infinite conductivity ($\sigma \rightarrow \infty$)

$$\frac{\partial \mathbf{B}}{\partial t} = \nabla \times (\mathbf{v} \times \mathbf{B})$$
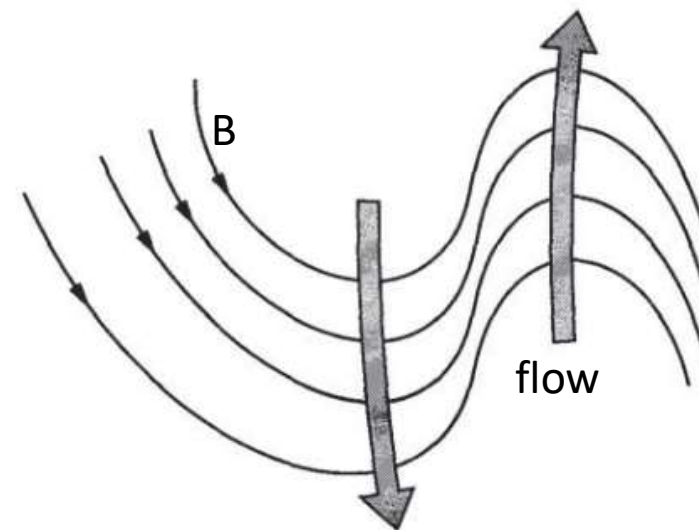
or equivalent

$$\mathbf{E} + \mathbf{v} \times \mathbf{B} = 0$$

Hydromagnetic theorem:

In infinitely conductive plasma, the total magnetic

induction encircled by a closed loop remains unchanged

-> magnetic field lines are "frozen" into the plasma flow

B

flow

Frozen magnetic field lines

Magnetic merging and reconnection

Back to the case of finite conductivity (both advection and diffusion terms present)
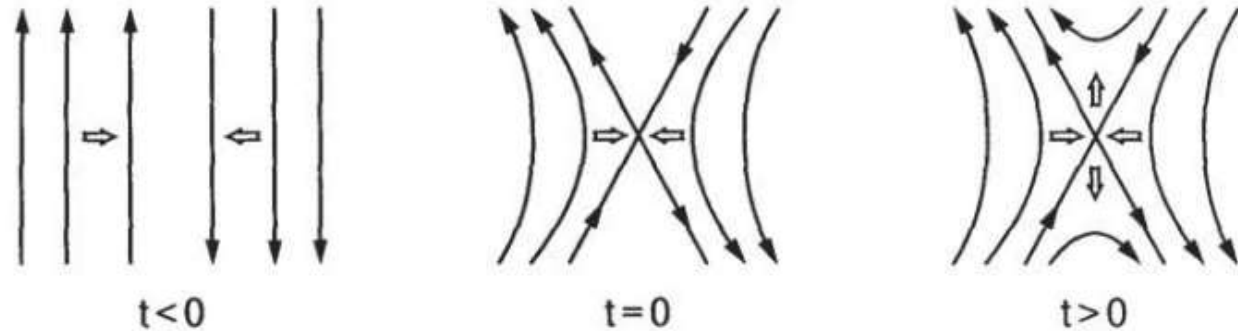
$$\frac{\partial \mathbf{B}}{\partial t} = \nabla \times (\mathbf{v} \times \mathbf{B}) + \frac{1}{\mu_0 \sigma_0} \nabla^2 \mathbf{B}$$

or in dimensionless form

$$\frac{B}{\tau} = \frac{V B}{L_B} + \frac{B}{\tau_d}$$

Magnetic Reynolds number

$$R_m = \mu_0 \sigma_0 L_B V$$

t<0   t=0   t>0

Magnetic field line merging

For $R_m \gg 1$: diffusion is negligible (in solar wind $R_m \approx 10^{17}$)

For $R_m \sim 1$: diffusion is substantial and can dominate -> merging/reconnection

Interplanetary magnetic field (IMF): Parker spiral

- Solar rotation drags out frozen solar wind magnetic field forming **Parker spiral** (after Gene Parker)

- Winding angle depends on wind speed, but on average

- ~ 45 deg at Earth orbit

- ~ 90 deg 10 AU

Orbit of Earth

300 km/sec

300 km/sec   300 km/sec

300 km/sec
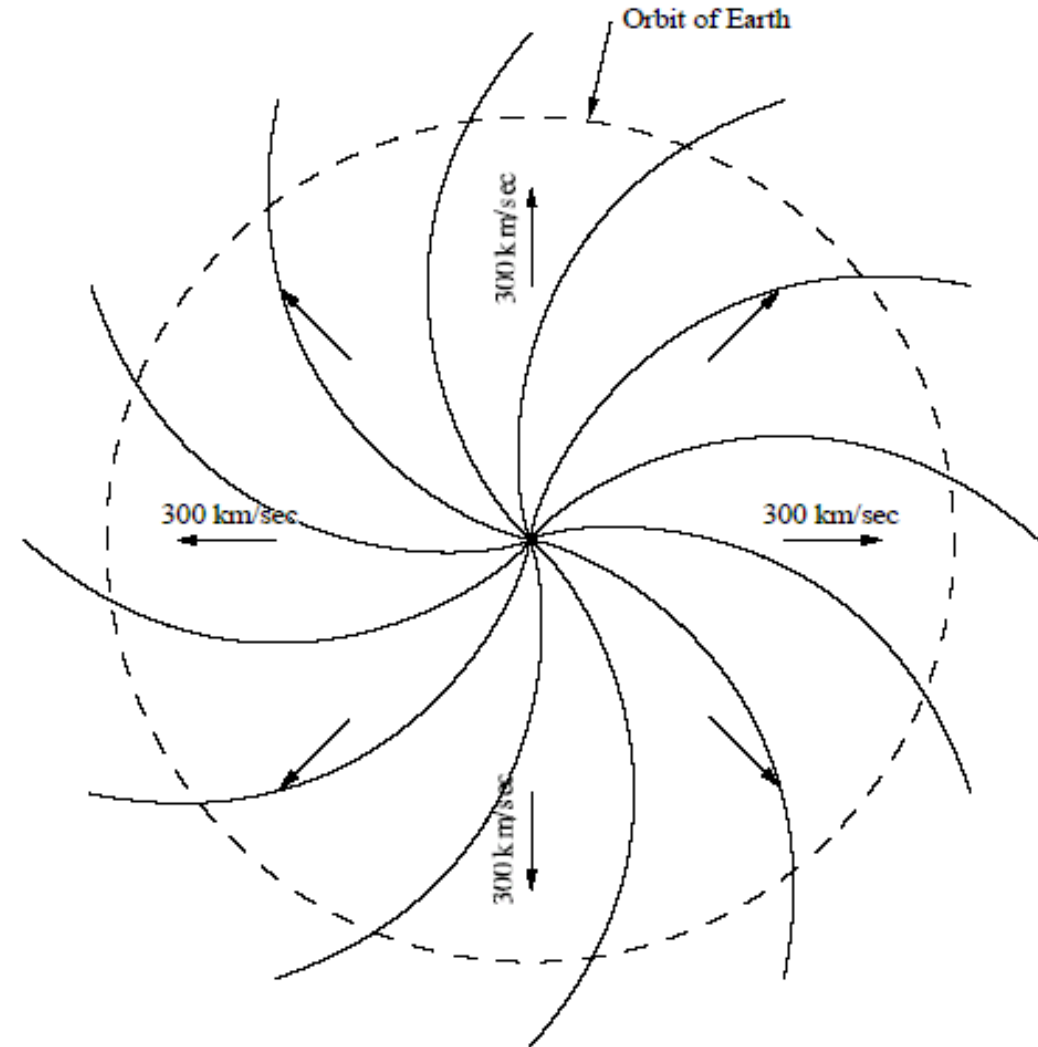
Earth's Magnetosphere

- Magnetosphere is the region of space where the Earth's own magnetic field dominates.
- Under southward IMF conditions, the merging of magnetic field lines is possible at the nose of magnetosphere (dayside reconnection).
- Closed magnetic field lines have both ends linked to the Earth; open field lines have one end linked to the solar wind.
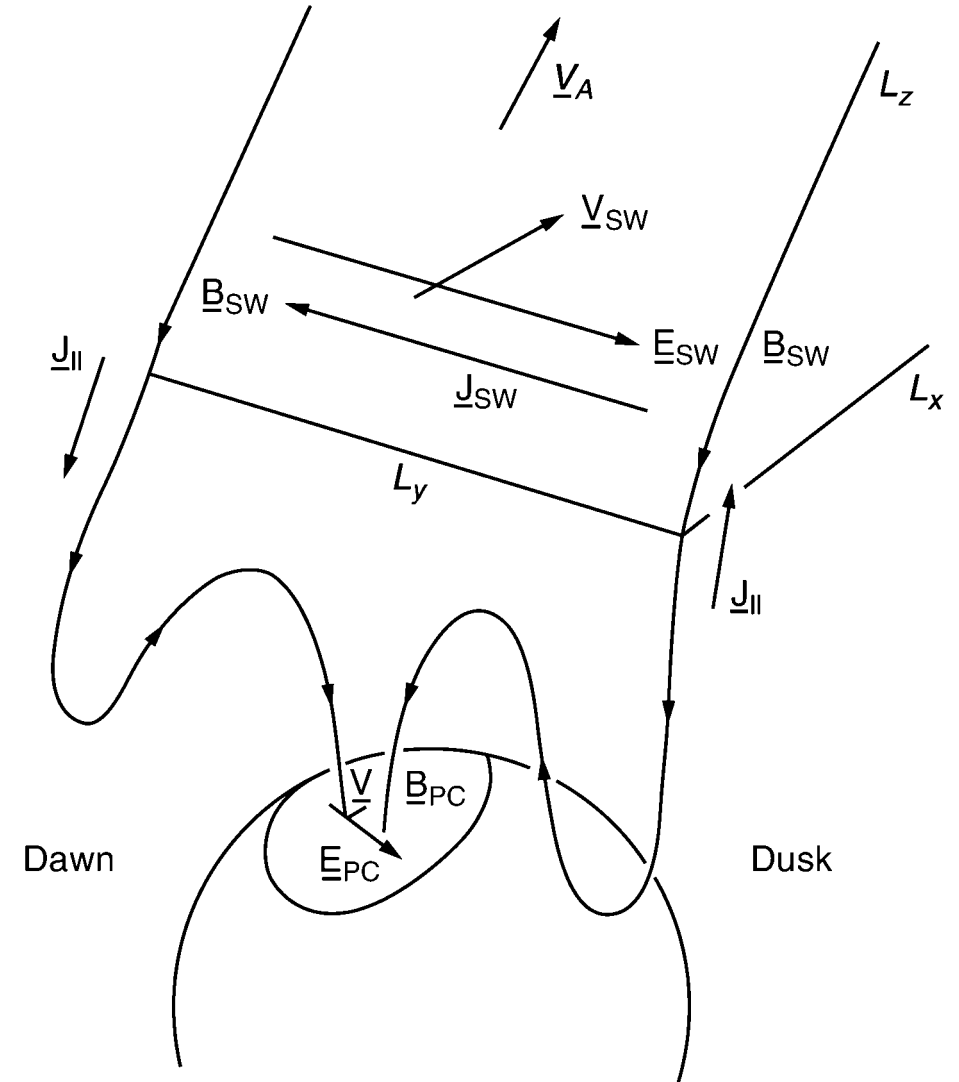

Courtesy of NASA
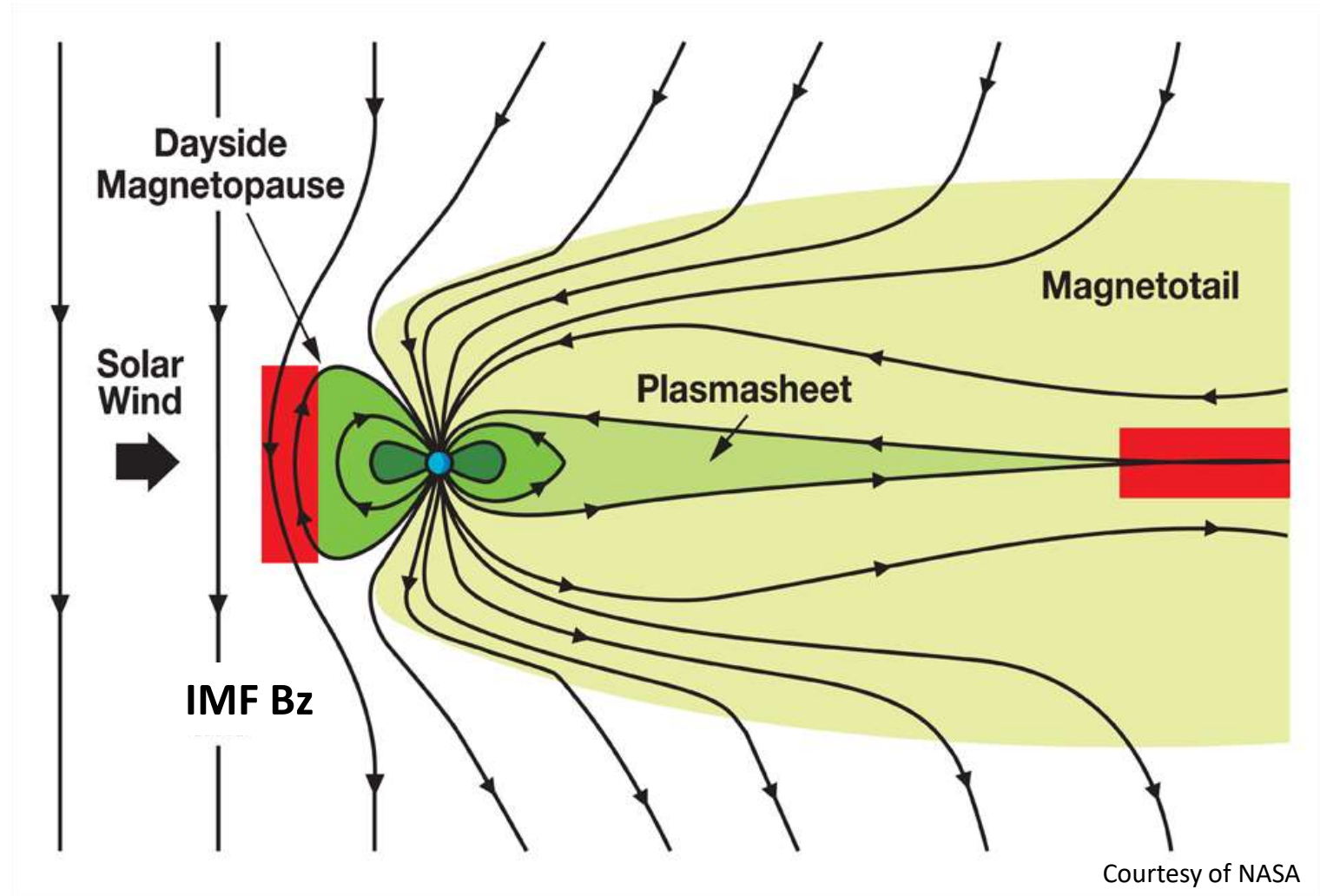
Coupling under southward IMF

Solar wind electric field (frozen-in plasma)

$$\mathbf{E}_{sw} = -\mathbf{V}_{sw} \times \mathbf{B}_{sw}$$

Under a southward IMF, a dawn-to-dusk solar wind electric field $\mathbf{E}_{sw}$ maps to the polar cap ionosphere.

Satellite navigation systems

GPS system

~ 30 navigational GPS spacecraft

55° inclination orbits

Broadcast two frequencies in L1 and

L2 bands (1.57 and 1.23 GHz).

Other similar GNSS systems:

GLONASS, Galileo, Beidou

Ionosphere is a dispersive media

Total electron content (TEC) along the signal path

from GPS spacecraft to the receiver can be inferred

by measuring the phase advance and/or the group

delay between different frequencies.
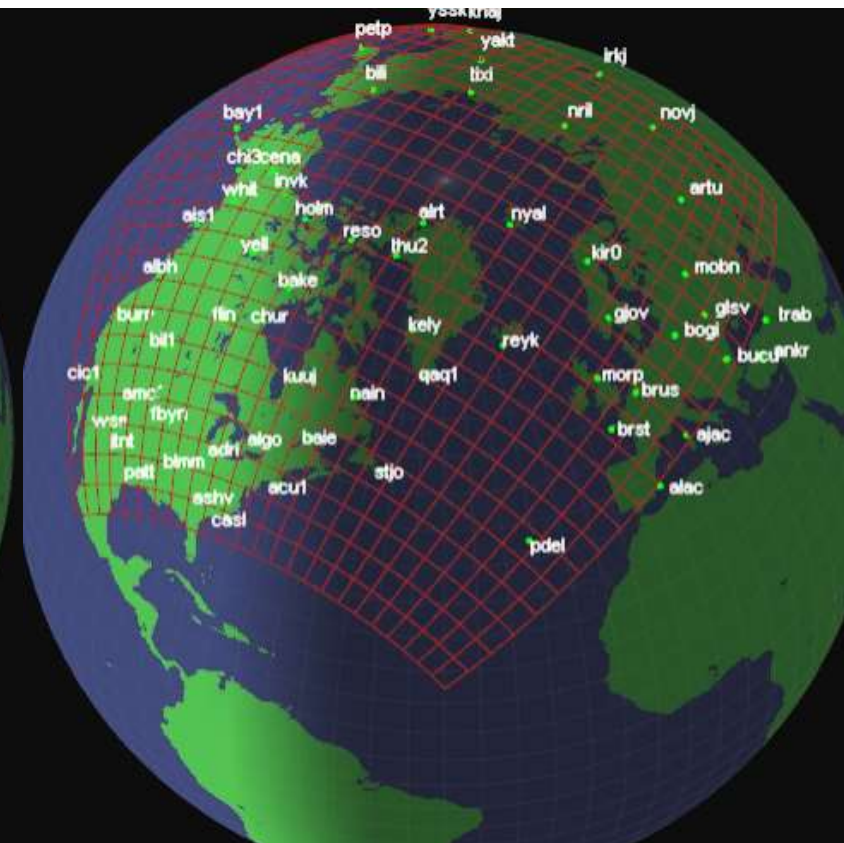
GNSS tomography example-1

Network of ground dual-frequency GNSS receivers at high latitudes.

Tomographic inversion of the GNSS data should reveal plasma dynamics.
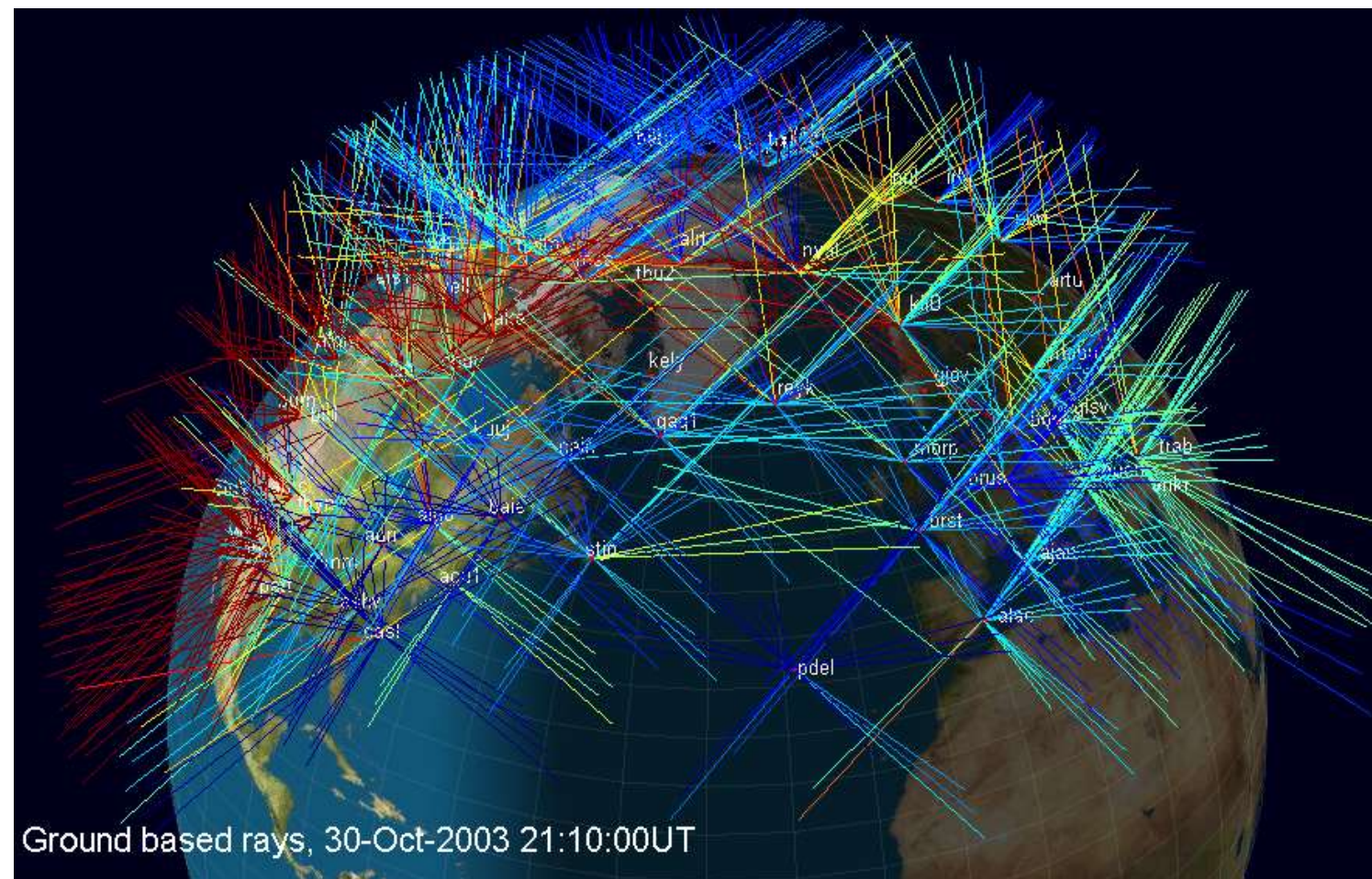

Network of GNSS receivers

Projection of the tomographic grid

GNSS tomography example-2

Rays of GPS signals received during the major 30-Oct-2003 geomagnetic storm.

Colour shows plasma content along the ray.


Ground based rays, 30-Oct-2003 21:10:00UT

GNSS tomography example-3

Results of the tomographic reconstruction: plasma density

The global distribution of ionospheric plasma density can be deduced from characteristics of GPS signals acquired by ground-based network of GPS receivers.

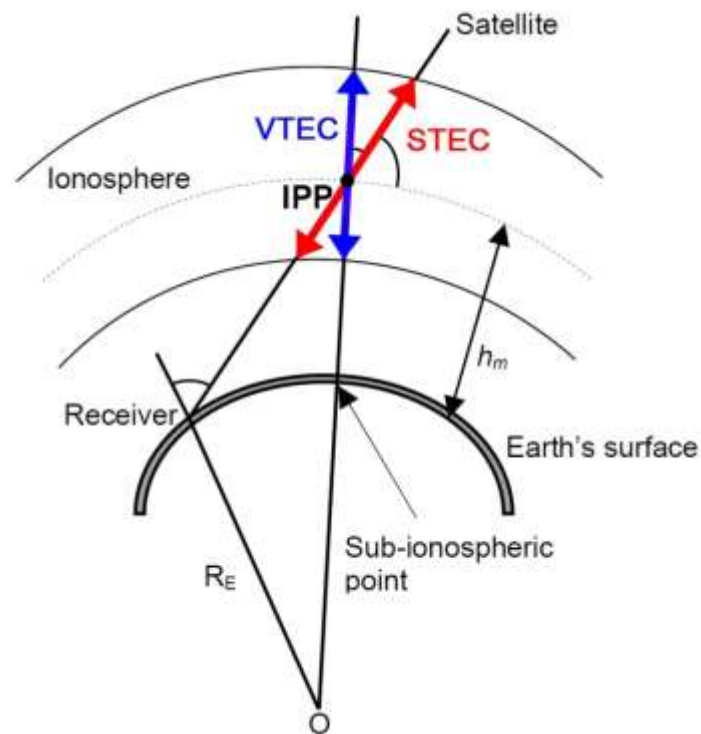Plasma follows general anti-sunward cross-polar convection.

Oct 30 2003, 21:00UT
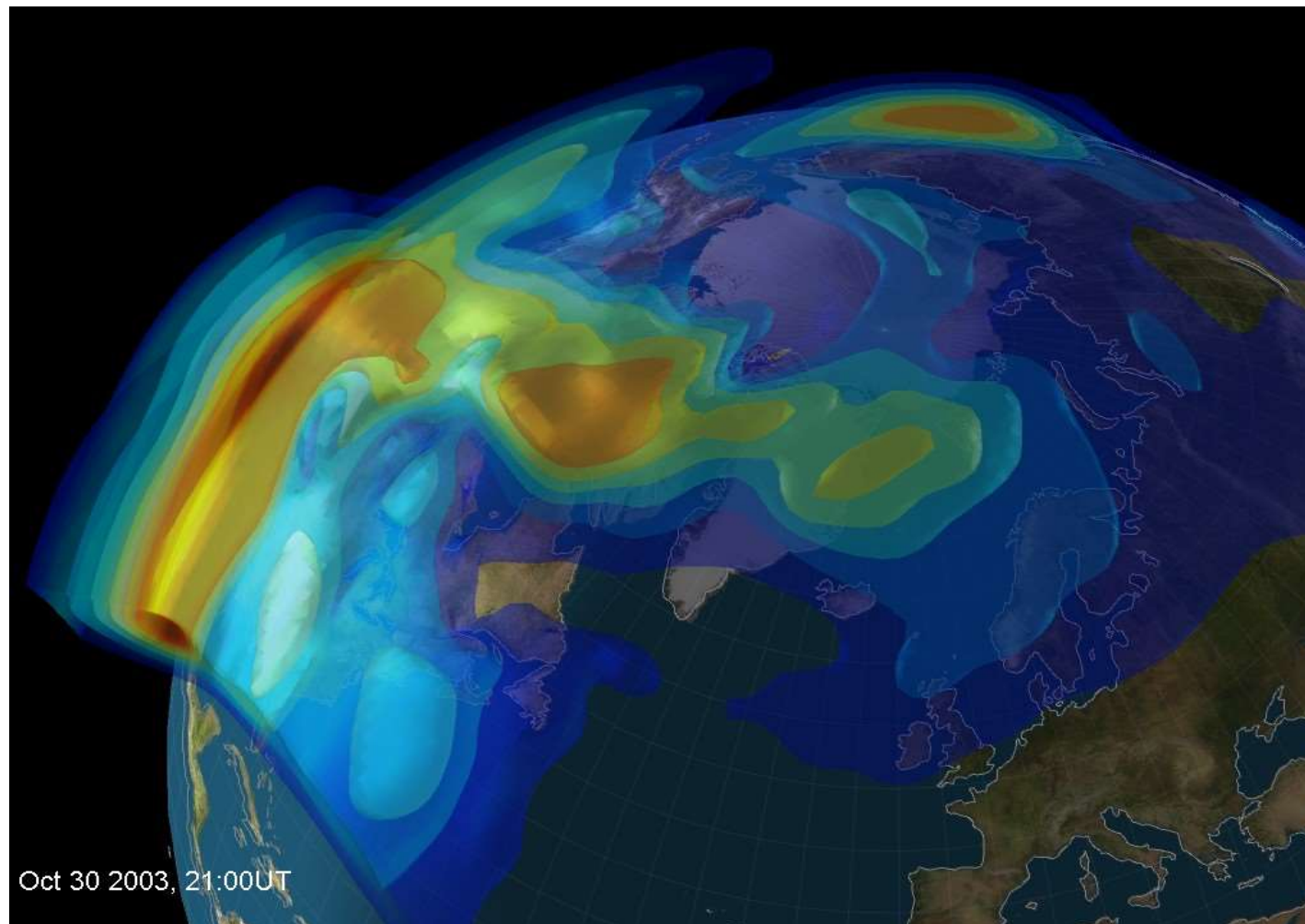
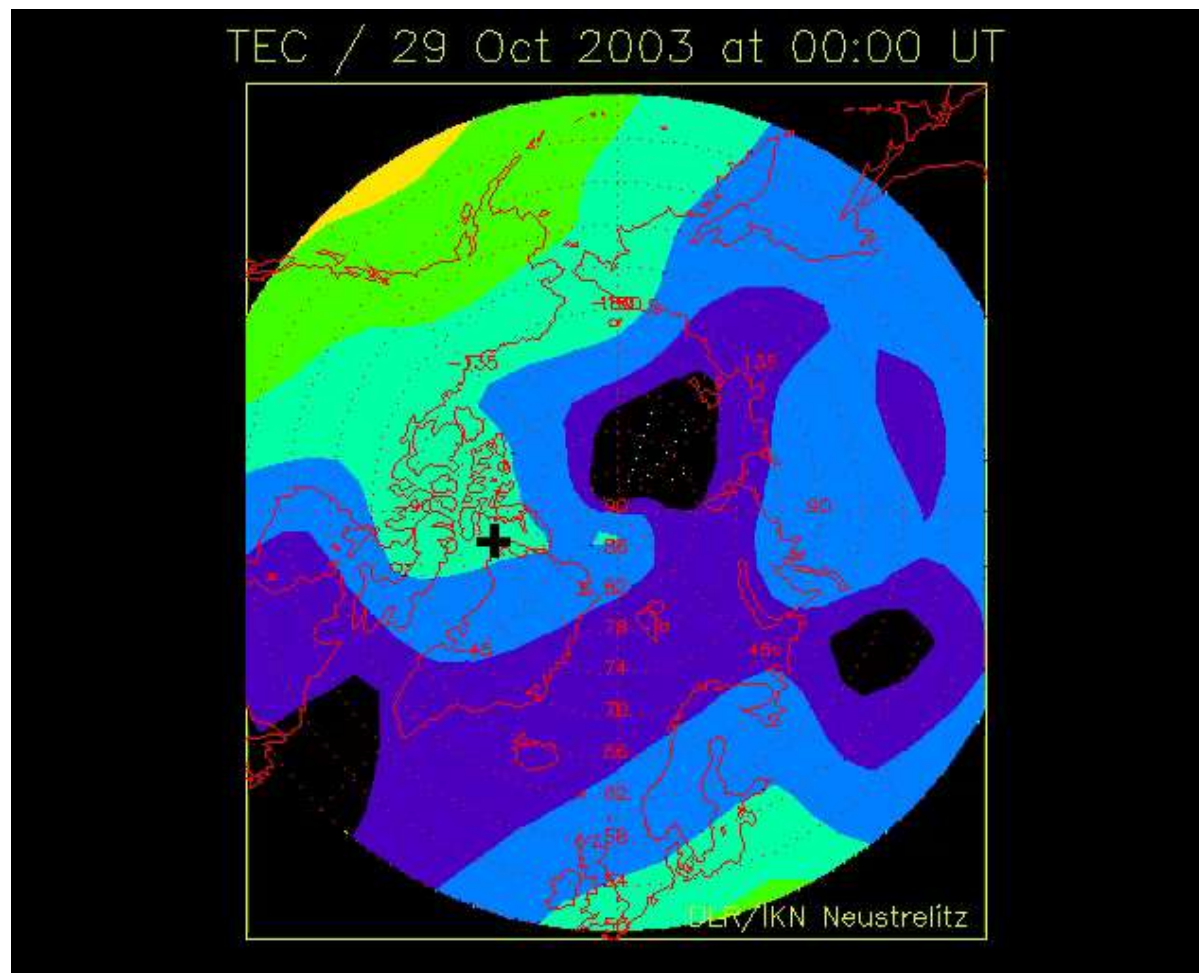Mitchell et al, AGU Mono. 2008, doi:10.1029/181GM09

DLR

Direct reconstruction of TEC

Simpler direct reconstructions are also possible.

Only assumptions about ionospheric equivalent height (centre of mass) are needed.


From Jaacob et al., 2008

Jakowski et al., JASTP, 2008, doi:10.1016/j.jastp.2005.02.023

Fromation of polar tongue of ionisation during storms

- Neutral winds can push plasma along (up) the field lines, to where the plasma recombination rate is slower.

- ExB drift may have a vertical component at mid-latitudes.

- Other mechanisms (e.g., chemical or compositional changes) could be more important during storm recovery phases.
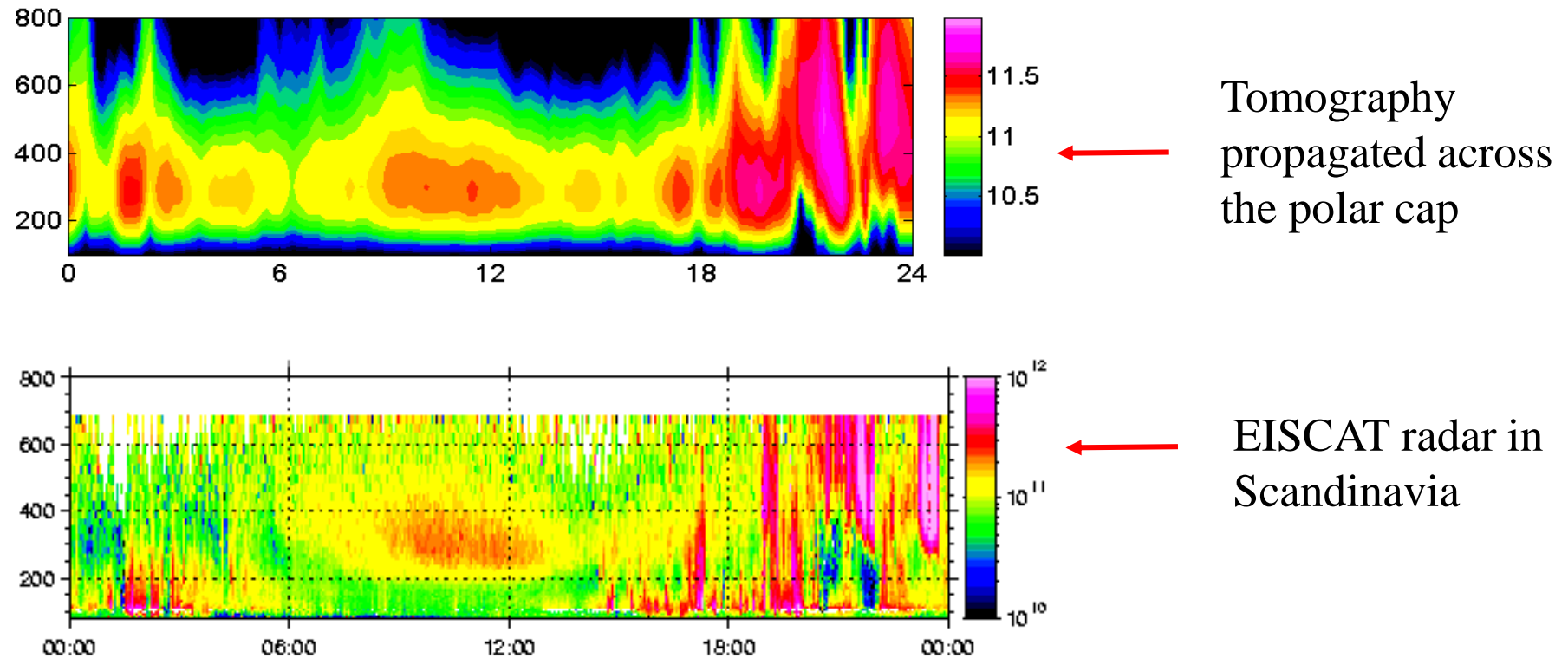

Foster et al., 2005, doi:10.1029/2004JA010928
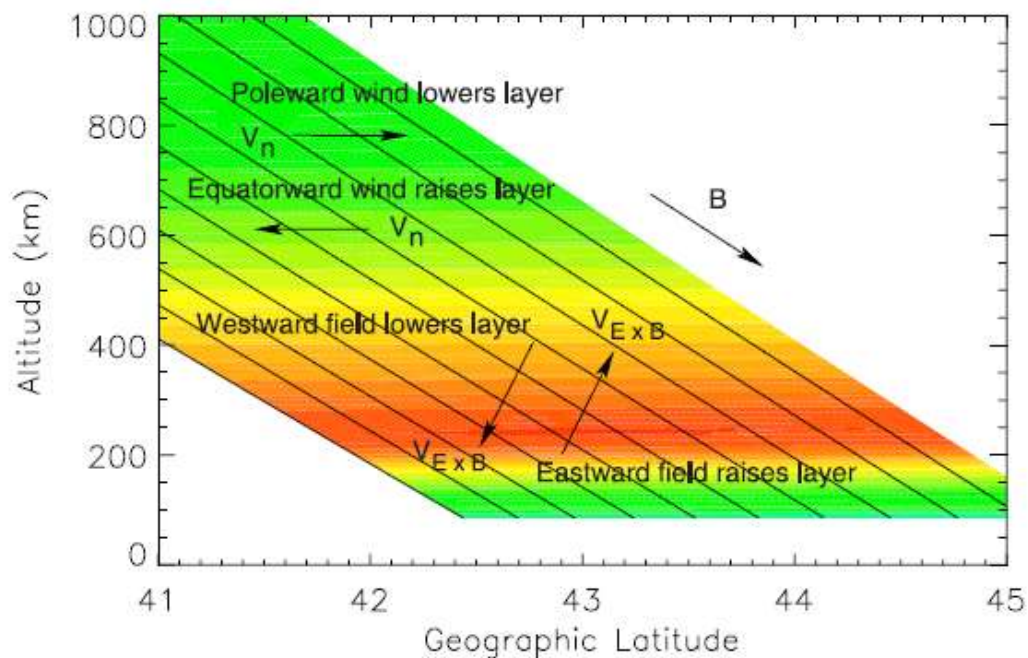
Swisdak et al., 2006, doi:10.1029/2005GL024973

DLR
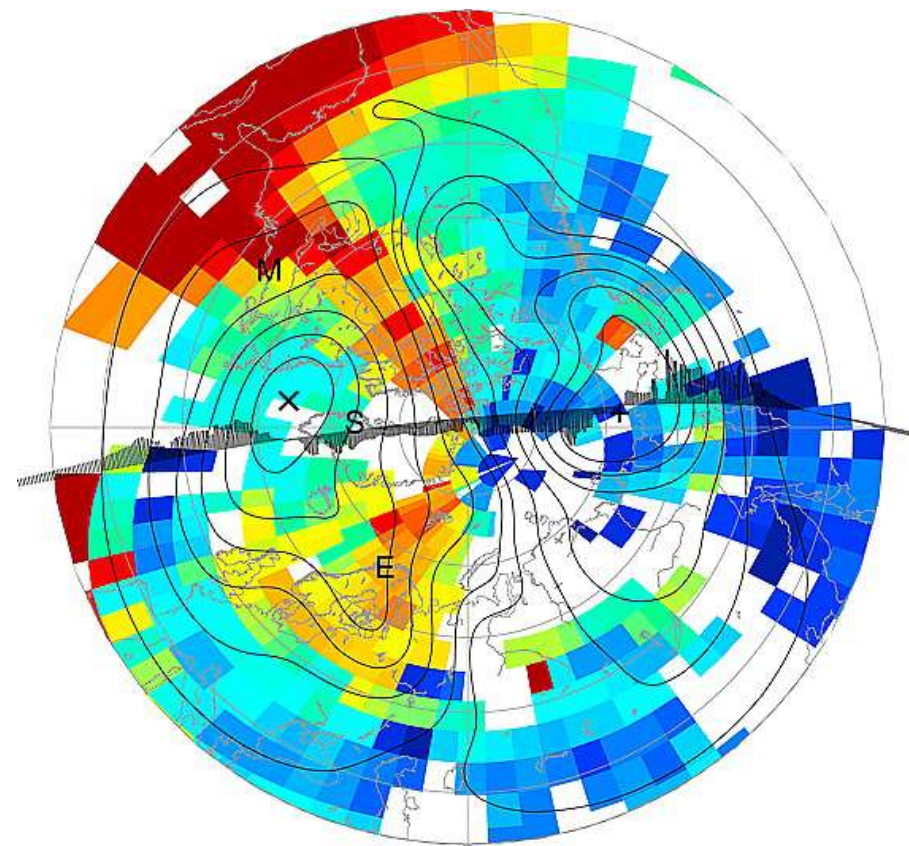
Comparison with ground radar observations

Electron density during 30-Oct-2003 storm as a function of height and UT

Tomography propagated across the polar cap

EISCAT radar in Scandinavia

Mitchell et al., 2008, doi:10.1029/181GM09

Example: 20-Nov-2003 geomagnetic superstorm

- The storm is isolated with a quiet pre-storm day (19-Nov).

- Formation of the high-latitude anomaly is expected during the main phase (12 - 21UT).

- The tongue would be forming in North American sector (dayside during the main phase) spreading anti-sunward.

- More on the 20-Nov-2003 superstorm:
  - Foster et al., 2005, doi:10.1029/2004JA010928
  - Pokhotelov et al., 2008, doi:10.1029/2008JA013109
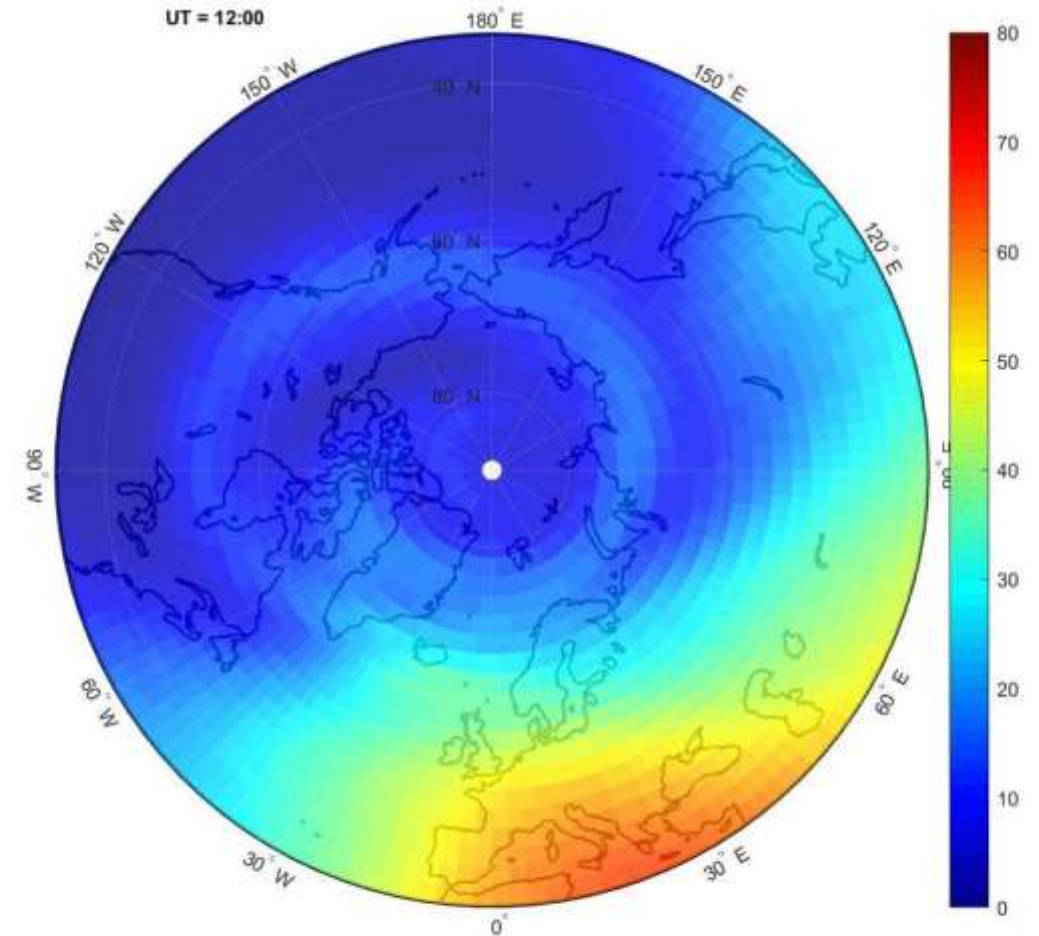 - Pokhotelov et al., 2021, doi:10.5194/angeo-39-833-2021
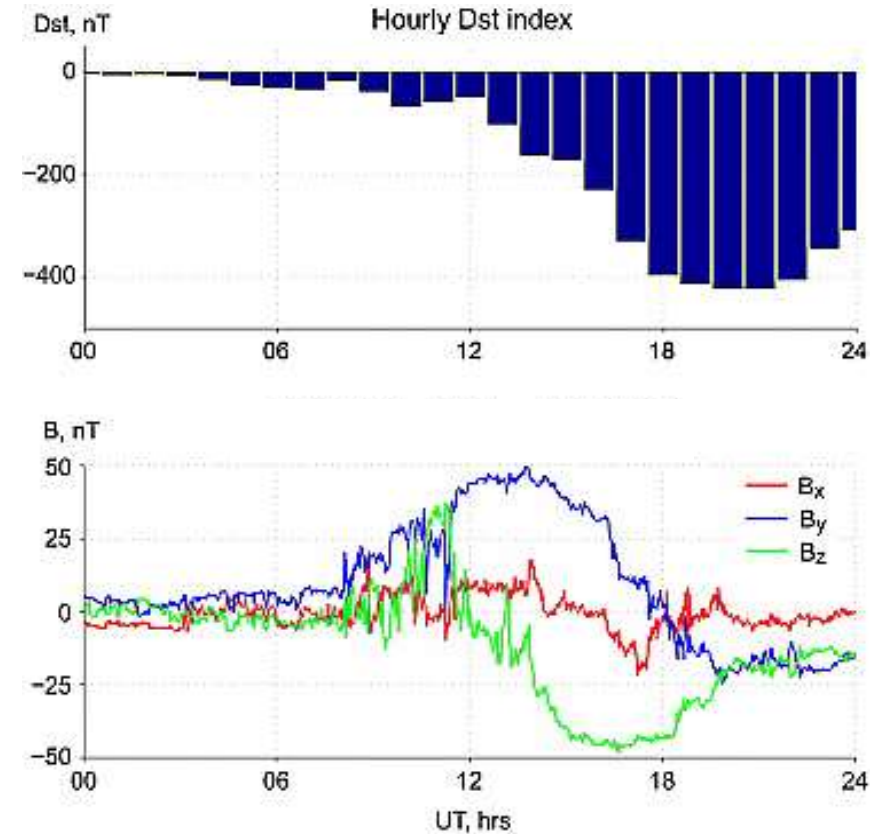
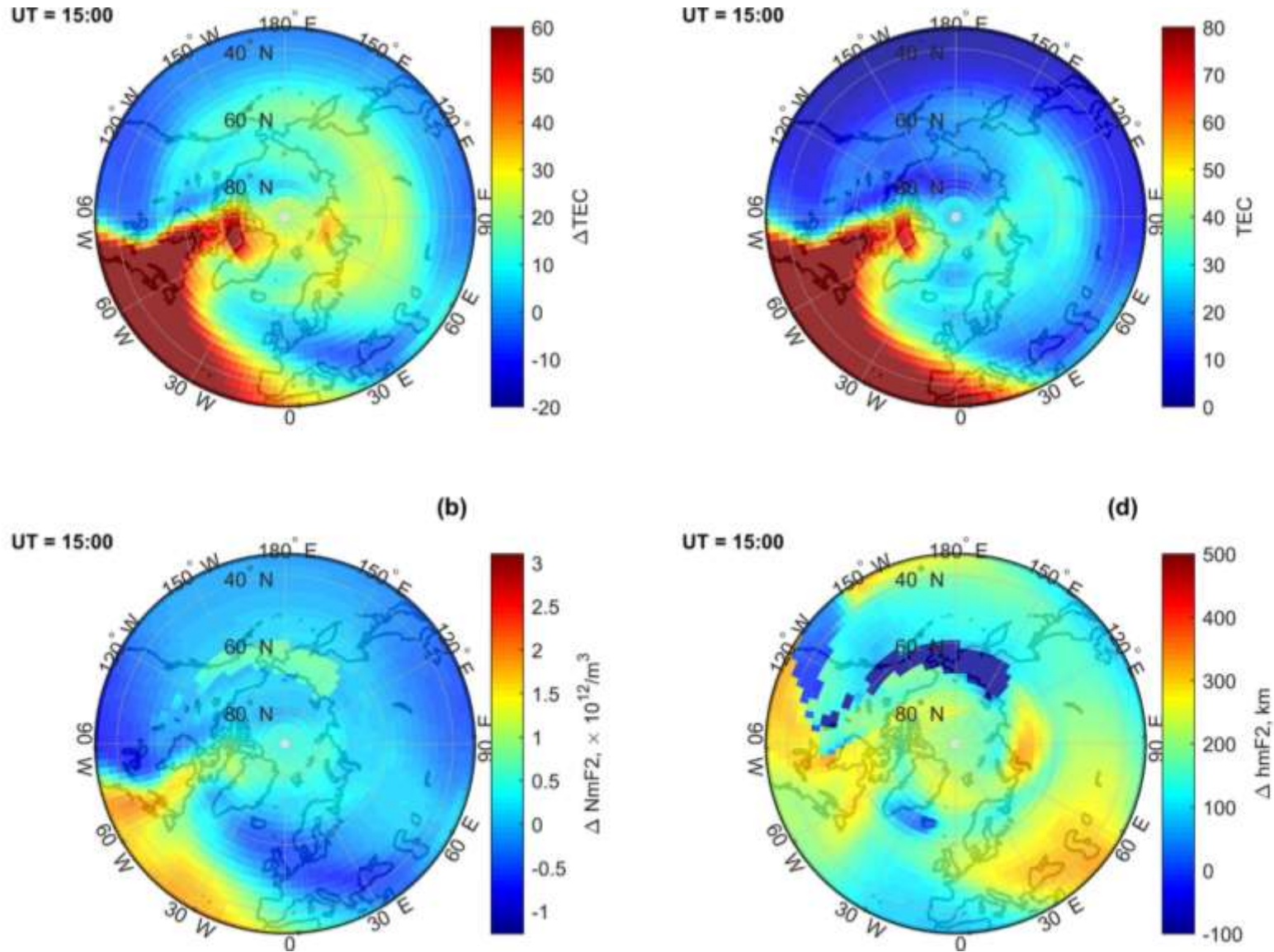Pokhotelov et al., 2008
doi:10.1029/2008JA013109

TIE-GCM Simulations: polar cap view

- TIE-GCM simulation of the TOI with Weimer model.

- Animated polar projections (above 30°N).

- TOI maximises over North American Atlantic sector during the main phase (16-18 UT).

- At 18-20 UT large amounts of transported plasma reach over the polar cap into Scandinavian sector.
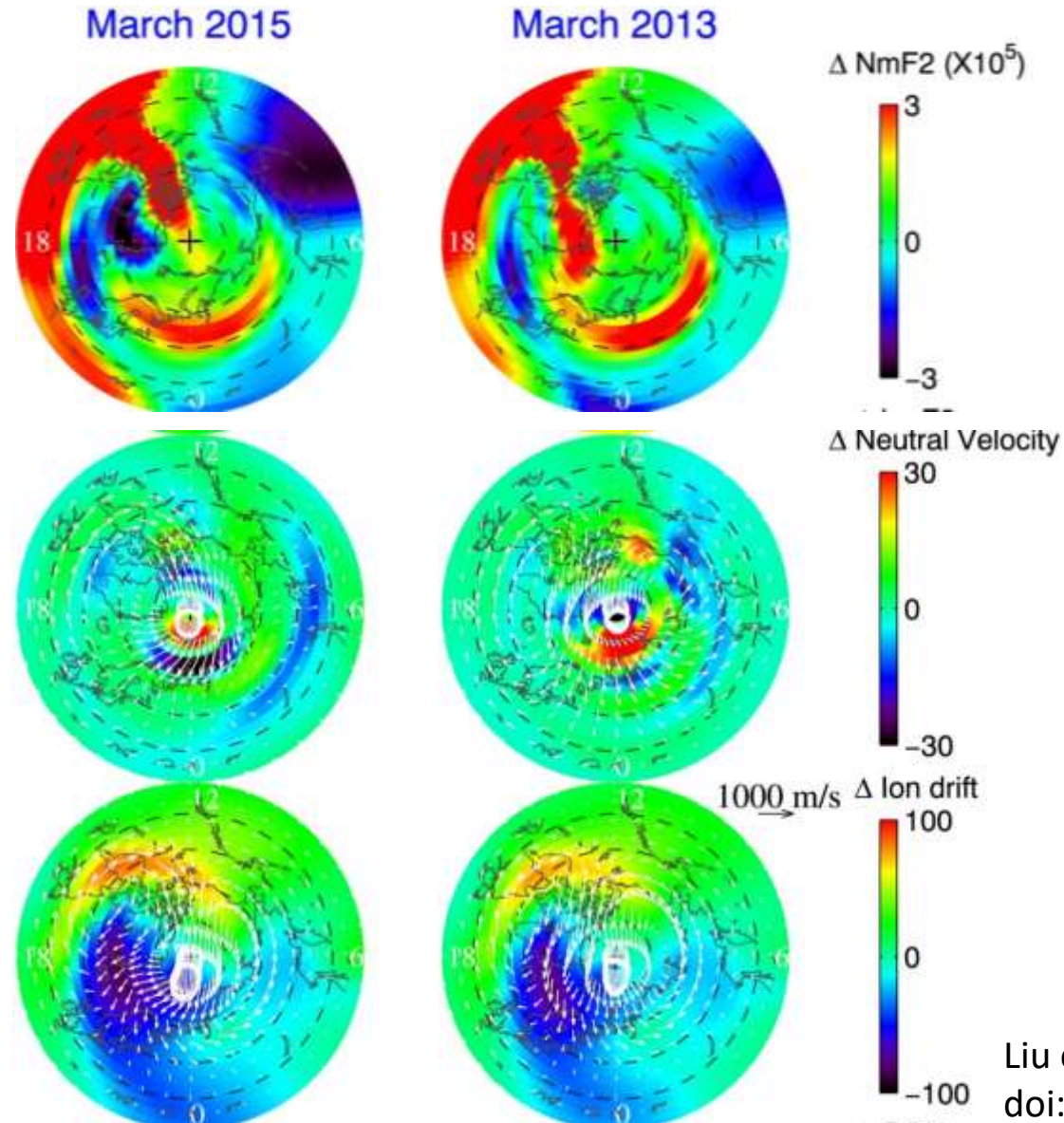

Pokhotelov et al., 2021, doi:10.5194/angeo-39-833-2021

TEC and simulated ionospheric heights from TIEGCM

Comparison to the simulations of different geomagnetic storms

March 2015   March 2013

$\Delta NmF2 (X10^5)$

Δ Neutral Velocity

Δ Ion drift

1000 m/s

- TIE-GCM simulation of the TOI with Weimer ExB transport model for Mar 2015 (left) and Mar 2013 (right) storms.
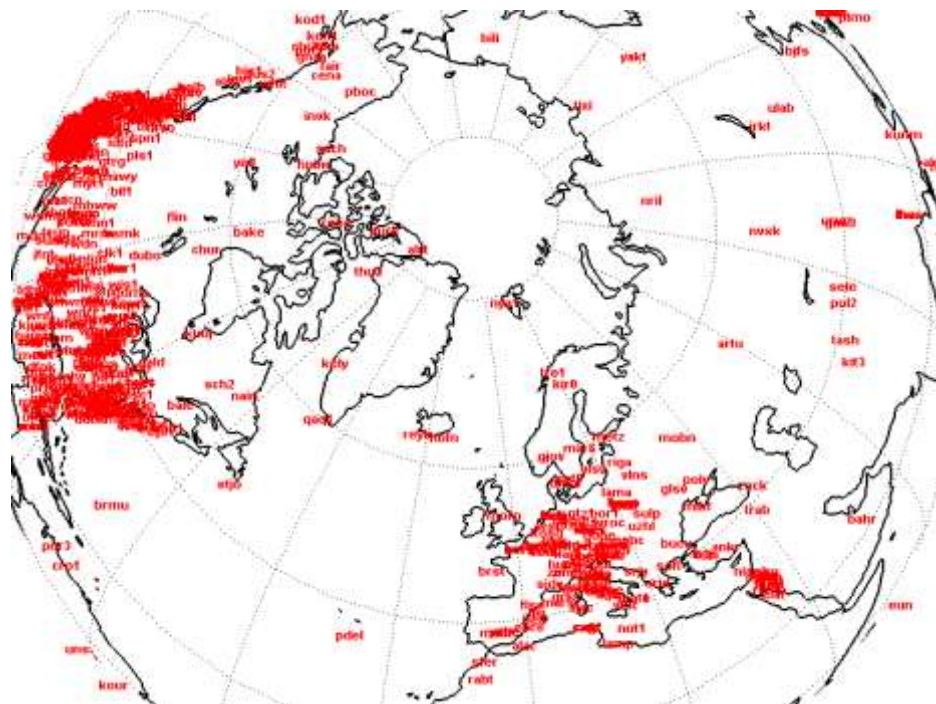
- Geomagnetic storms of different origins:
  - CIR- and HSS-driven storms: Pokhotelov et al., 2009 doi:10.1029/2009JA014216; 2010 doi:10.1098/rspa.2010.0080

Liu et al., JGR, 2016
doi:10.1002/2016JA022882

DLR

Ground networks of GNSS receivers

Global scale

- IGS network distributed over the globe.

- Coverage varies greatly with location.

Mesoscale

Dense networks of GNSS receivers in Fennoscandia

- 86 stations in Finland;

- over 200 stations in Sweden;

- more stations in Norway.

Ionospheric waves in GNSS and ISR data

20 January 2010; Tromsø; electron density filtered at period 1.05 h

Travelling ionospheric disturbances (TIDs) can be sensed simultaneously by EISCAT radar (vertical structure) and by GNSS receiver network (horizontal structure).

The analysis of GNSS data (~200 receivers in Sweden) was inspired by Japanese research (e.g., Tsugawa et al. 2004) on detecting ionospheric effects from extra-long "pre-tsunami" waves.
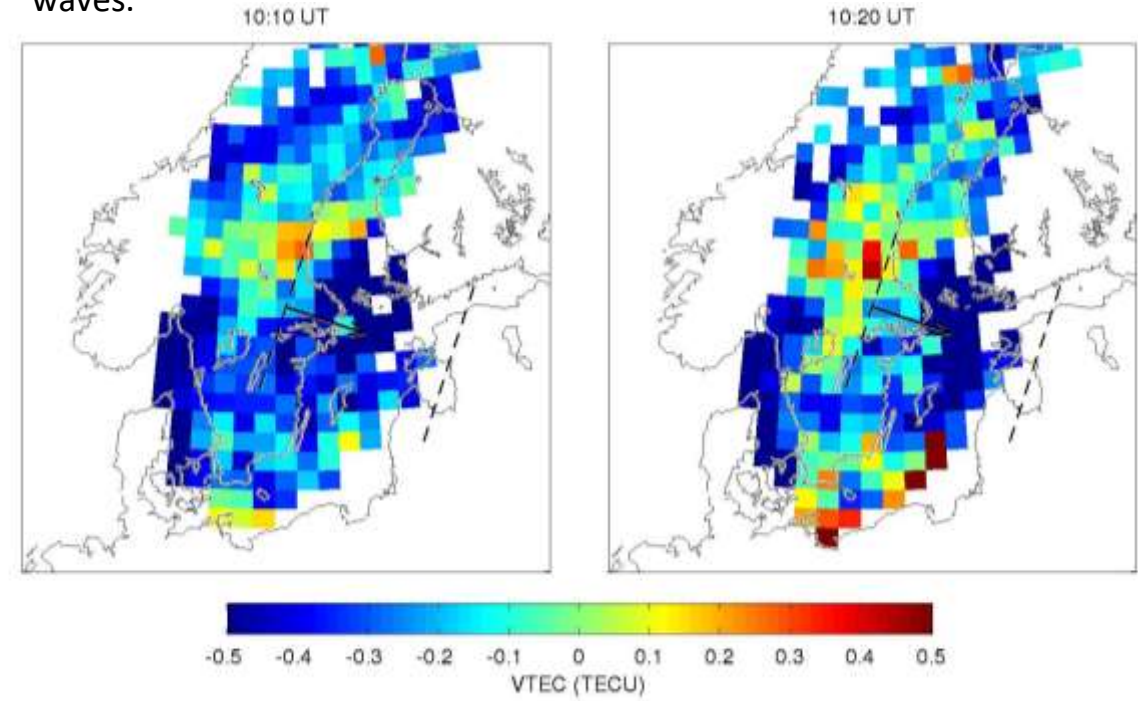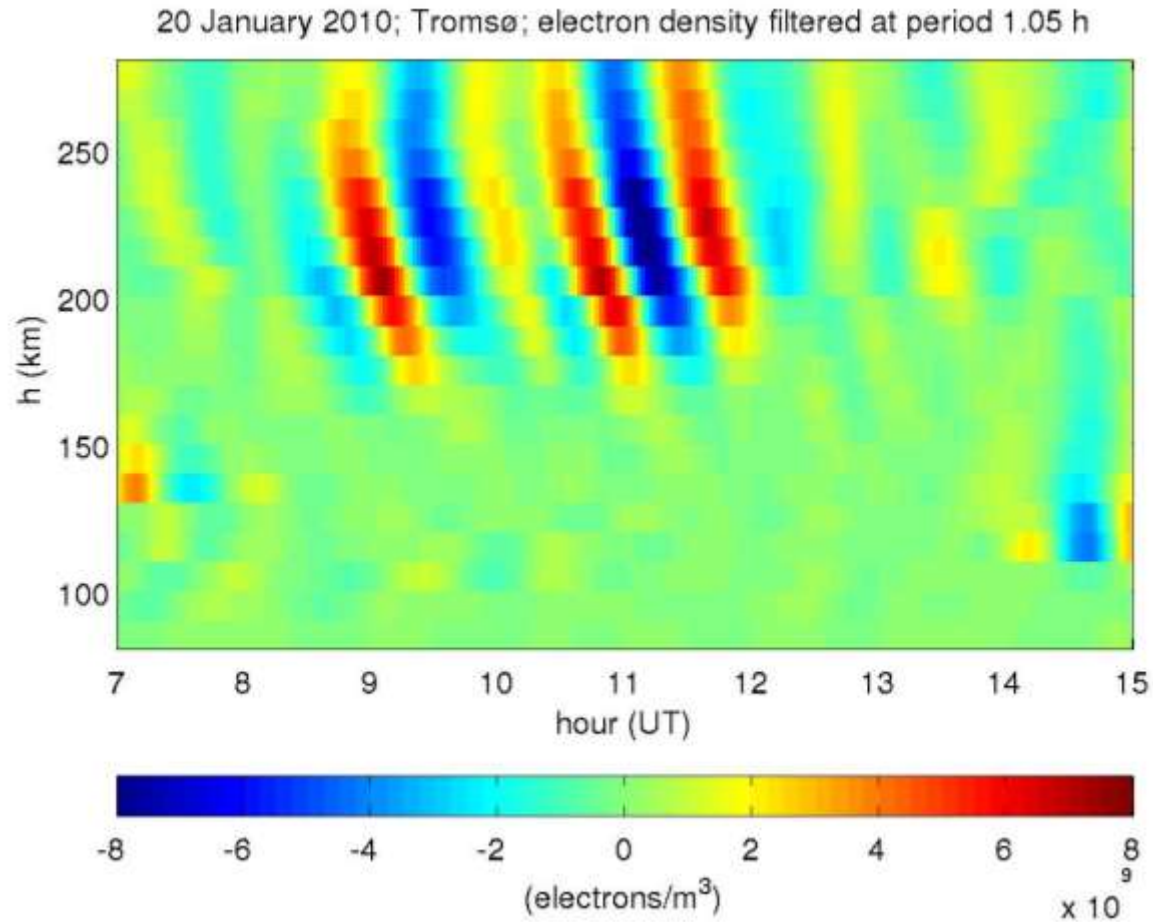
van de Kamp et al, 2014 doi:10.5194/angeo-32-1511-2014

SAR imaging of auroral ionosphere
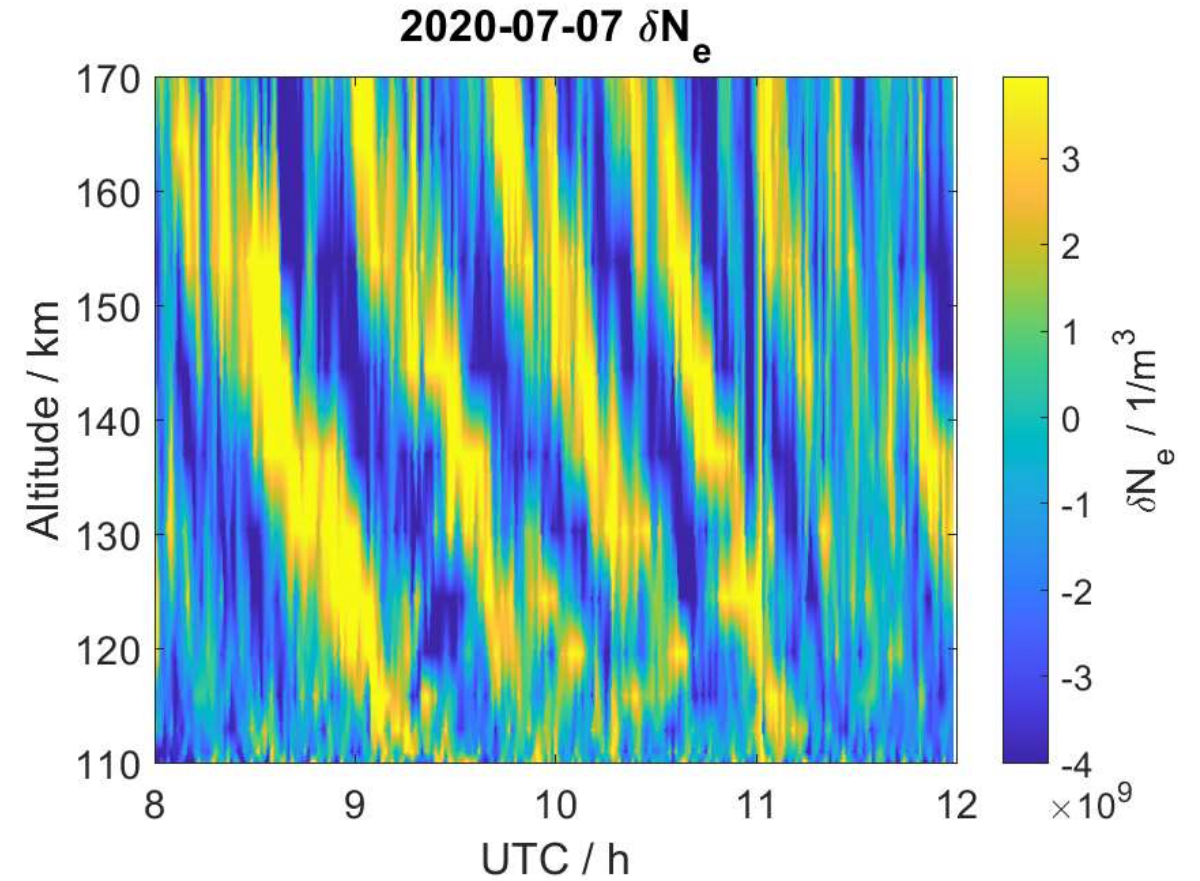
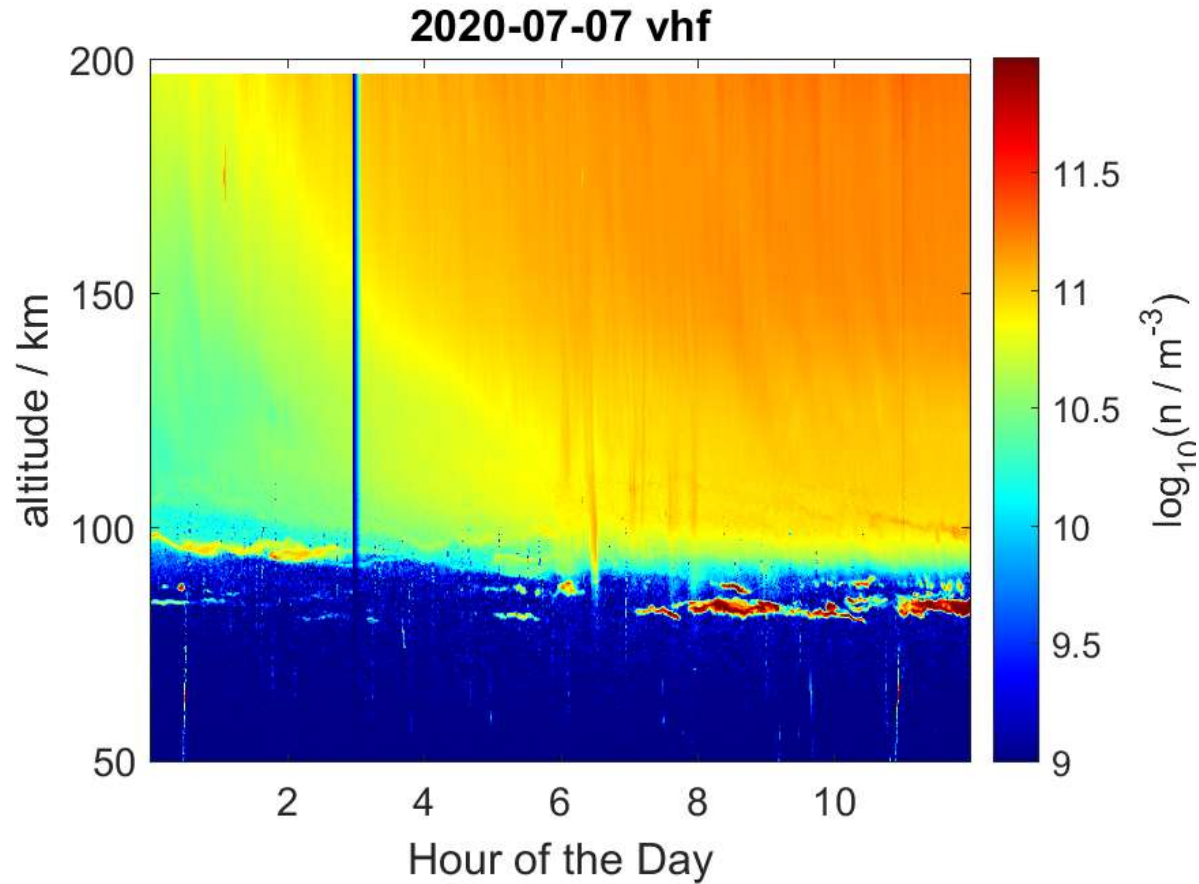Imaged TEC irregularities
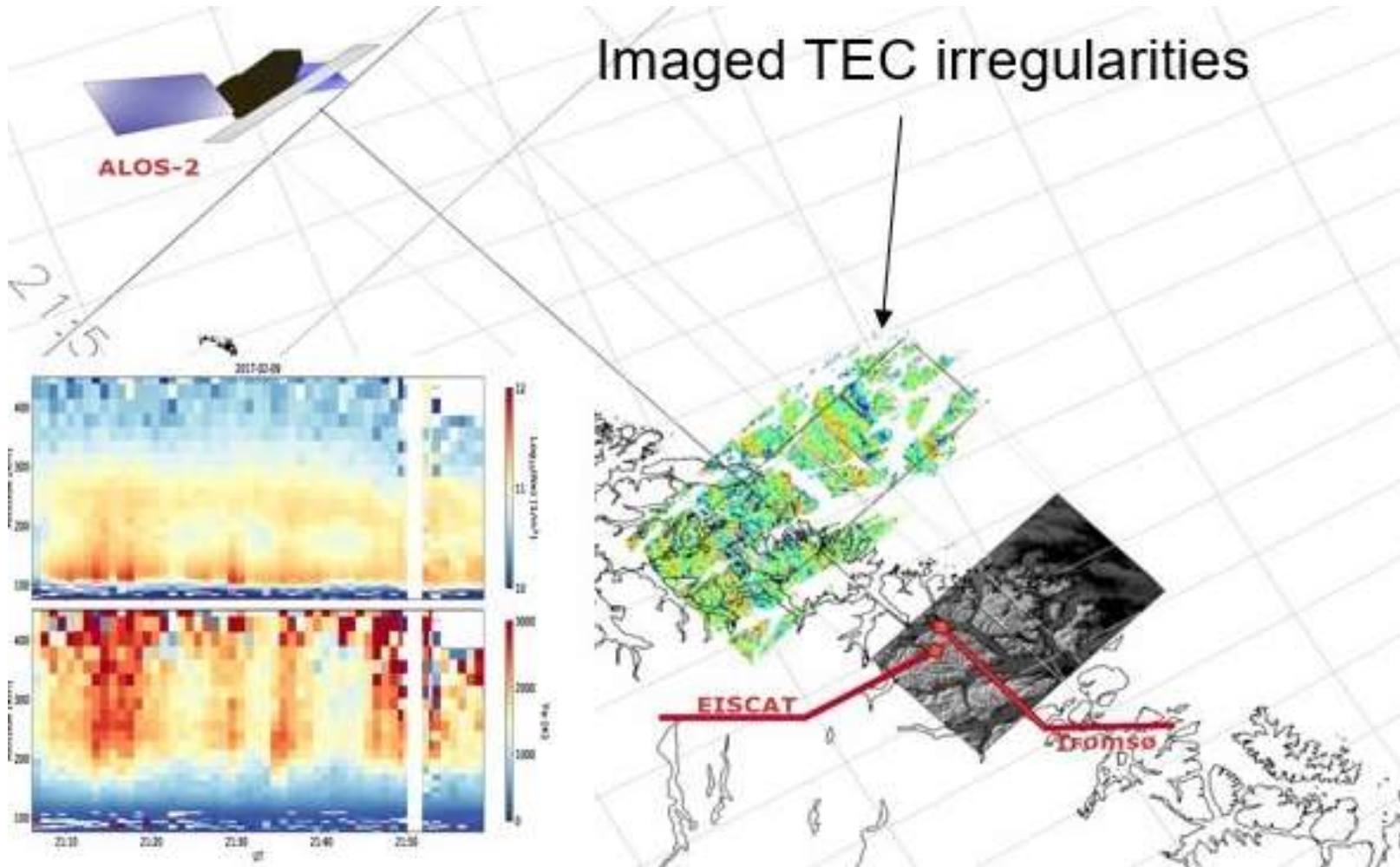
Synthetic Aperture Radar (SAR)

Imaging high-latitude plasmaImaging high-latitude plasma density irregularities resulting from particle precipitation: spaceborne L-band SAR and EISCAT observations.

ALOS-2

EISCAT

TROMSØ

Sato et al., 2018, doi:10.1186/s40623-018-0934-1

DLR

Neutral winds and TIDs from EISCAT

2020-07-07 vhf

2020-07-07 δN_e

**Bistatic EISCAT experiment from 2020
(jointly with Univ. of Bern and Univ of Tromsoe)**

Günzkofer et al., in preparation

Frictional heating theory, models and measurements

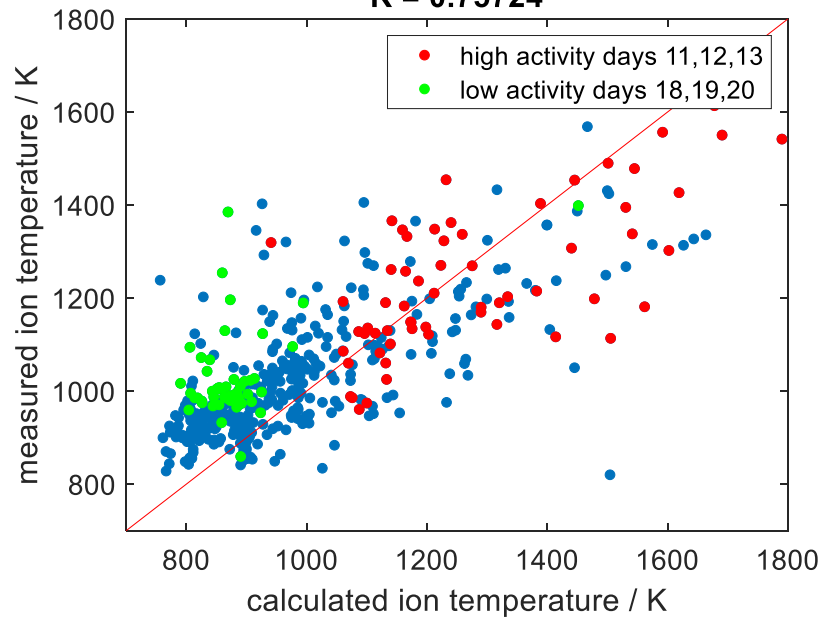$$T_i = T_n + \frac{m_n}{3k}(u_i - u_n)^2 = T_n + \frac{25}{3} \cdot 10^{-4} \cdot (u_i - u_n)^2$$

$$\frac{m_n}{3kB^2} = 0.33 \cdot 10^6$$

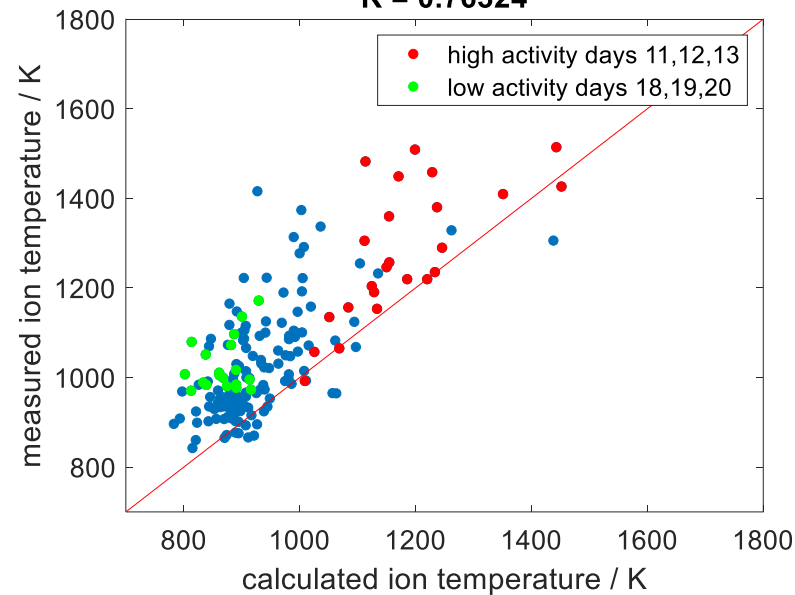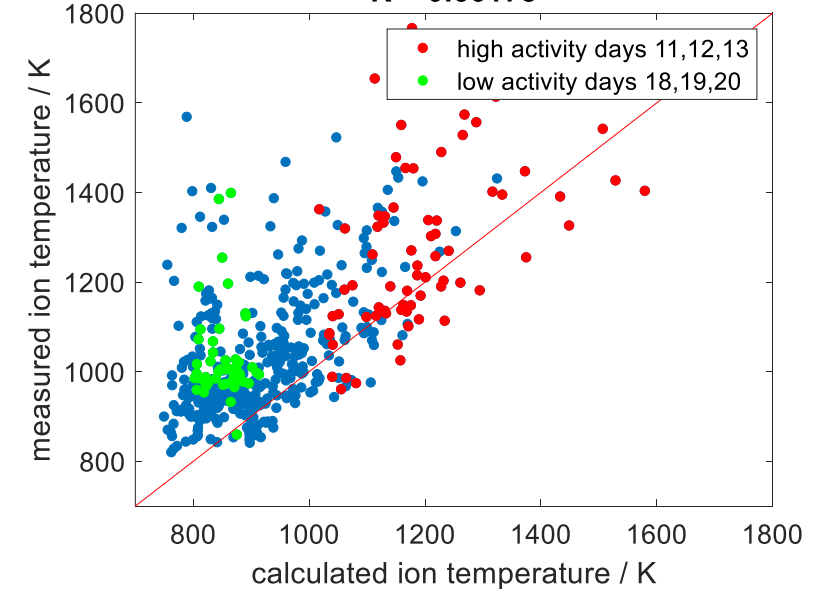$T_n; u_n$: model neutral atmosphere

at 300 km

u_i: EISCAT

u_i: WACCM-X SD

u_i: TIE-GCM

Günzkofer et al., in preparation

Summary: neutral dynamics issues

- There seem to be a mismatch between polar cap neutral winds, produced by different circulation models (WACCM-X, GAIA, etc.).

- Number of earlier works (e.g., Burns et al., 2004; Liu et al., 2016) suggested that neutral winds during geomagnetic storms blow generally anti-sunward across the polar cap, following much faster plasma drifts.

- The anti-sunward neutral wind can be due to enhanced ion drag imposed by the ion drifts.

- An efficiency of such drag mechanism needs to be validated, especially at lower altitudes of the transition region (~120km).

DLR

Summary: plasma dynamics issues

- There is a mismatch between polar cap ExB plasma convection, produced by different convection models (Heelis, Weimer, SuperDARN, AMIE, etc.), especially in the extent of how far the ExB convection expands during geomagnetic storms.

- Electrodynamic transport plays the dominant role in the storm main phase, in the recovery phase a complex interplay between different mechanisms is involved.

- Relative roles of co-rotational and convectional forces are poorly understood.

- Mechanisms of plasma uplifts at middle (sub-auroral) latitudes need to be understood, but difficult to measure. Mid-latitude SuperDARN and/or incoherent scatter radars should be used.

References

- Jakowski et al, JASTP, 2007 https://doi.org/10.1016/j.jastp.2005.02.023

- Mitchell, Yin, Spencer, Pokhotelov, AGU Monograph 181, 2008, https://doi.org/10.1029/181GM09

- Pokhotelov et al., JGR, 2008 https://doi.org/10.1029/2008JA013109

- van der Kamp, Pokhotelov, Kauristie, AG, 2014 https://doi.org/10.5194/angeo-32-1511-2014

- Sato, Kim, Jakowski, Häggström, EPS, 2018 https://doi.org/10.1186/s40623-018-0934-1

- Pokhotelov, Fernandez-Gomez, Borries, AG, 2021 https://doi.org/10.5194/angeo-39-833-2021

- Günzkofer, Pokhotelov, et al., JGR, 2022 https://doi.org/10.1002/essoar.10511964.1 (preprint)

Further info and the current presentation for download:

https://www.researchgate.net/profile/Dimitry-Pokhotelov